A Two-Step Approach for Forecasting Wind Speed at Offshore Wind Farms During Typhoons

Xuan Liu[1(✉)] and Jun Guo[2]

[1] Energy and Electricity Research Center, Jinan University, Zhuhai 519070, Guangdong, China
xliu514@gmail.com

[2] State Key Laboratory of Disaster Prevention and Reduction for Power Grid Transmission and Distribution Equipment, State Grid Hunan Electric Power Company Disaster Prevention and Reduction Center, Changsha 410007, Hunan, China

Abstract. Wind power has become the leading factor in the transition from fossil fuels to renewable energy sources. The total capacity of offshore wind farms in China has increased significantly in the past decade. It's essential to understand the risk posed by typhoons to offshore wind farms. However, the impacts of typhoons are hard to predict due to the limited number of observations. In this study, a deep learning-based two-step approach is proposed for estimating the wind speed of given locations during typhoons. An LSTM-based seq2seq model is implemented in the first step to predict the typhoon track and intensity. In the second step, a linear wind field model is adopted to calculate the wind speed at specific locations. The case study results show that the proposed approach is capable of predicting the extreme wind speed at specific offshore locations during typhoons. This study demonstrates the potential of assessing wind risk with a combination of data-driven and physics-based models.

Keywords: Wind Speed Prediction · Offshore Wind Farm · Typhoon · Neural Network · LSTM · Seq2seq

1 Introduction

Due to the global climate crisis, the energy industry is transitioning from fossil fuels to renewable energy, such as wind and solar. In 2005, China introduced the Renewable Energy Law, which changed the global wind energy market significantly. By the end of 2015, China has installed one-third (33.5%) of global wind power [1]. It's worth noting that offshore wind quality is better than onshore

Supported by the Open Project Funding of State Key Laboratory of Disaster Prevention and Reduction for Power Grid Transmission and Distribution Equipment.

H. Yang et al. (Eds.): SmartGIFT 2022, LNICST 483, pp. 95–107, 2023.
https://doi.org/10.1007/978-3-031-31733-0_9

wind quality. The power output of an offshore wind turbine is expected to be 1.7 times the same onshore wind turbine [2]. The offshore wind resources are abundant in China's coastal area. By the end of 2020, China's offshore wind farm installation accounts for more than 50% of the global installed offshore wind farm capacity [3].

Unlike onshore wind farms, offshore wind farms are exposed to more natural hazards, such as extreme wave heights and Tropical Cyclones (TCs). TCs are one of the most severe natural hazards responsible for massive damage and causalities in coastal areas. TCs come with strong winds and thunderstorms and are the leading cause of floods and storm surges in coastal regions. Structures are highly vulnerable to typhoons when the wind speed exceeds the design limits, while storm surges are the deadliest effect of TCs, causing 90% of TC deaths historically [4]. TCs are referred to as Typhoons in the Western North Pacific basin. According to the State Oceanic Administration of China (SOA), the long-term average of annual direct economic losses is about $2.6 billion from 1989 to 2017. Moreover, studies show that the average typhoon intensity is increasing due to global warming [5]. Therefore, an effective tool for predicting the wind speed at critical locations during typhoons is necessary and urgent for the risk mitigation, management, and decision-making of wind farms.

Thanks to the presence of satellites, TCs can be tracked accurately anywhere in the world. TC track forecasting has improved substantially during the past few decades. According to the National Hurricane Center (NHC), the average 24h TC track forecast error has dropped from ∼130 nmi to ∼30 nmi [6]. The cyclone forecast models can be categorized into four main categories: statistical models, numerical models, ensemble models, and deep learning models.

Statistical models are based on the statistical analysis of historical cyclone information instead of explicitly considering the physics of tropical cyclones. This type of model is relatively simple to compute compared to the more complex models that consider the physics of the atmosphere but is also less accurate due to its simplicity. The climatology and persistence (CLIPER) model, first developed in 1972 [7], is a statistical regression model considering the non-linear relationship between input predictors and the predictands. Errors of the CLIPER model are often used as a baseline for other forecast models. Linear autoregressive models that only consider the current and previous translation speeds and directions are also shown to be plausible [8] for track generation. Vickery et al. [9] suggest that the translation speed and direction are interdependent and depend on the cyclone location.

Numerical models, also known as dynamical models, are highly complex and require supercomputers to process the mathematical equations governing the physics and motion of the atmosphere. Dynamical models come with different resolutions: the global models calculate the atmospheric variables of the entire earth, while the regional models only calculate the variables in a limited area. An example of a global model is the Global Environmental Multiscale Model (GEM) [10] developed by the Canadian Meteorological Centre (CMC). GEM has a variable-resolution capability so that it can also produce high-resolution

regional forecasts. In operational applications, GEM runs the output for up to 10 days to provide medium-range and short-range forecasts.

Ensemble models (or consensus models) combine multiple forecasting results to produce better-quality results. The ensemble can consist of either multiple forecasts from a single base model or different models. In the single-base-model approach, a single numerical model is initialized with a set of different initial conditions to generate a set of forecasts for the ensemble. Monte Carlo Simulation [11,12] is shown to be a plausible initialization method. Krishnamurti et al. [13] suggest that a physical initialization method, which entails the assimilation of observed rain rates in a numerical model, could reduce the variance of an ensemble forecast with one single base model. However, single-model ensembles are rarely used in current operational applications since they are not as effective as multi-model ensembles. In multi-model ensembles, the forecasts of all ensemble members are usually weighted to reduce the bias in the final predictions. The multi-model ensembles are shown to be capable of providing significantly better track predictions than individual models [14].

In recent years, deep learning has been proven to be a powerful tool in cyclone behavior modeling. Alemany et al. [15] utilize Recurrent Neural Network (RNN) to predict TC trajectories and show that the performance is comparable to the NHC official forecasts in a grid-based system. However, the error of the RNN-based model increases significantly when converting the grid location to latitude and longitude coordinates. Giffard-Rosin and Yang [16] combine Convolutional Neural Network (CNN) and Multi-Layer Perceptron (MLP) to extract features from multimodal source data and feed the extracted features to a fusion network to predict the 24-forecast cyclone displacement. The results show that the proposed model has lower forecast errors on all basins than BCD5, a benchmark statistical model.

The existing forecasting models mainly focus on predicting the track or intensity of the TCs. These models can not be directly used to assess the wind speed at given offshore wind farms during typhoons. In this study, a two-step model that utilizes both the deep-learning technique and cyclone physics is proposed. The model takes the initial typhoon condition (the current and previous track location and intensity) as input and produces the wind speed predictions at given observation locations. The main contribution of this study can be described as follows:

- Feature extraction methods, including geographical representation, storm velocity, and grid transition probabilities, are used during data preprocessing to extract interpretable explicit features from raw data.
- A two-step approach is proposed to predict wind speed at given locations during typhoons. An LSTM-based seq2seq model is developed as the first step of the proposed approach. The seq2seq model predicts the future typhoon trajectory based on the initial typhoon condition. After that, a linear boundary layer wind model is employed in the second step to calculate the wind speed at given locations.

– The proposed approach is validated using measurement data gathered from a real-world offshore wind farm. The results suggest that the proposed method is capable of predicting wind speed accurately at given offshore wind farms during typhoons.

The rest of the paper is organized as follows: Sect. 2 describes the training data and the preprocessing method for the proposed model. The proposed two-step approach is presented in Sect. 3. In Sect. 4 the case study based on real-world data is discussed. Section 5 concludes.

2 Data Preprocessing

The raw track data comes from the CMA Tropical Cyclone Best Track Dataset [17,18], which covers tropical cyclones that develop over the Western North Pacific. The records in the dataset contain the storm IDs and names, date and time of the record, storm intensity category, storm location (storm center latitude and longitude), minimum pressure near the storm center, and 2-min mean maximum sustained wind speed near the storm center. However, about 10% of the entries in the dataset don't have valid 2-min mean maximum sustained wind speed records. Therefore, only the storm location and minimum pressure near the storm center data were used to construct the feature space for the track forecasting model in step 1. The dataset provides 3-hourly data for the landed typhoons since 2017, while most of the data are 6 h apart. Since the track forecasting model makes predictions in 6-h intervals, only data that are 6 h apart were used in this study.

2.1 Geographical Representation

The latitude and longitude coordinates of the storm locations are transformed into pairs of x and y coordinates using Lambert's Conic Conformal (LCC) Projection [19]. The LCC-transformed coordinates make better geographical representations of the cyclone track since the conic projections reduce the distortion associated with the spherical coordinate system at higher latitudes and maintain the geographic shapes.

2.2 Storm Velocity

The geographic coordinate sequences obtained from the raw track dataset are non-stationary. Therefore, the storm velocity is calculated to de-trend the sequences. The storm velocity is represented by the storm translation direction and speed. The translation direction (θ) and speed (c) are calculated using the Haversine formula:

$$\Delta\phi_i = \phi_i - \phi_{i-1} \tag{1}$$

$$\Delta\lambda_i = \lambda_i - \lambda_{i-1} \tag{2}$$

$$a_i = \sin^2\left(\frac{\Delta\phi_i}{2}\right) + \cos\phi_{i-1} \cdot \cos\phi_i \cdot \sin^2\left(\frac{\Delta\lambda_i}{2}\right) \tag{3}$$

$$c_i = 2 \cdot R \cdot \arctan\left(\sqrt{\frac{a_i}{1-a_i}}\right) / \Delta t \tag{4}$$

$$\theta_i = \arctan\left(\frac{\sin(\Delta\lambda_i) \cdot \cos\phi_i}{\sin\phi_i \cdot \cos\phi_{i-1} - \sin\phi_{i-1} \cdot \cos\phi_i \cdot \cos(\Delta\lambda_i)}\right) \tag{5}$$

where $R = 6371$ km is the earth radius and $\Delta t = 6$ h is the time difference between track records.

2.3 Grid Transition Probabilities

The cyclone track behavior is affected by many geographic-related features, such as surface roughness, height, and temperature. In order to better capture the spatial patterns influenced by geography, the grid transition probabilities are calculated based on historical data. First, a 0.7×0.7 degree grid network is created to cover all the tracks in the dataset. If a historical storm record is contained in a grid cell (i, j), the grid transition probability of the nearby $9 \times 9 = 81$ grid cells centered at grid cell (i, j) is then calculated as

$$p_{ij}(k) = \frac{n_k}{m_{ij}}, k = 1, 2, ..., 81 \tag{6}$$

where k is the index of the k_{th} associated cell centered at grid cell (i, j), n_k is the total number of records transit from cell (i, j) to the k_{th} associated cell in 6 h, and $\sum_1^m n_k = m_{ij}$.

2.4 Sliding Window

In many real-life applications (e.g., unit commitment), day-ahead forecasting is desired for forecasting models. Since each input record is 6 h from its previous record, one day is a sequence of length 4 in the track data. The training data is then generated using a sliding window of length 8 (4 for input and 4 for validation) on the original dataset.

2.5 Normalization

A min-max normalization is applied to features to make each input feature have equal scales:

$$x' = \left(\frac{x - \min(x)}{\max(x) - \min(x)} \right) \tag{7}$$

where x is the original feature value and x' is the normalized value. The range of the normalized features is $[0, 1]$.

After the data preprocessing, the final input features after preprocessing include the LCC transformed coordinates (x, y), the minimum central pressure p, the storm translation direction θ, and speed (c), and the transition probabilities.

3 Methodology

3.1 Problem Formulation

Definition 1. *Typhoon Track: A typhoon track X is composed of consecutive spatial temporal points $X = \{X_1, X_2, ..., X_T\}$. Each spatial temporal point X_i contains several parameters that essentially characterize the typhoon track: $X_i = [\lambda_i, \phi_i, p_{ci}]$, where λ_i, ϕ_i are the longitude and latitude coordinates of the typhoon center, and p_{ci} is the typhoon central pressure.*

Problem 1. Given a set of n observation locations $A = \{A_1, A_2, ..., A_n\}$ and a typhoon track $X = \{X_1, X_2, ..., X_T\}$, the goal is to predict the maximum sustained wind speed $V = \{V_1, V_2, ...V_n\}$ of each observation location in the next k time steps. The observation locations are defined by their geographic coordinates $A_i = (\lambda_i, \phi_i), i = 1, 2, 3, ..., n$, where λ_i is the longitude and ϕ_i is the latitude.

The problem is solved in two steps: First, the typhoon track information is fed into a deep neural network to generate a prediction of the typhoon track in the next k ($k = 4$ in this study) time steps. After that, a linear boundary layer wind field model is utilized to calculate the wind speed at each observation location based on the predicted track.

3.2 Seq2Seq Track Forecasting Model

The proposed approach utilizes a sequence-to-sequence (Seq2Seq) deep learning model to predict future typhoon locations based on the current typhoon track information. The techniques used in this model are described below:

Artificial Neural Network (ANN). ANNs are layered computing models inspired by the biological neural networks in human brains. A typical ANN consists of an input layer, one or more hidden layers, and an output layer. ANN is proven to be able to approximate any given function [20] and is capable of conducting time-series forecasting.

Recurrent Neural Network (RNN). RNN is a special class of ANN. The basic ANN models are not particularly good at processing sequence data since they assume that the data entries are independent. In RNNs, the output depends on not only the current input but also the output of previous data. This enables RNNs to capture the temporal dynamic behavior of time-series data.

Long Short-Term Memory (LSTM). Although RNNs work well with time-series data, they suffer from vanishing gradients and cannot catch the long-term relationships within the sequence data. LSTM is a variation of RNN that is specifically designed to solve the vanishing gradient problem. LSTM models utilize the "gate" mechanism to control the information flow. The gates are able to keep important information with a weight of 1. Therefore, long-term memory won't vanish anymore. The gates also have the ability to "forget" less important information to make the networks more efficient.

Seq2Seq Model. The Seq2Seq model is widely used in sequence-to-sequence tasks such as language translation and time-series forecasting. It utilizes the encoder-decoder architecture to process sequence data with variable lengths. The encoder-decoder architecture consists of an encoder and a decoder. The encoder transforms the input sequence into a fixed-shape state. The decoder maps the fixed shape state to a variable-length output sequence. Figure 1 shows the proposed seq2seq model architecture.

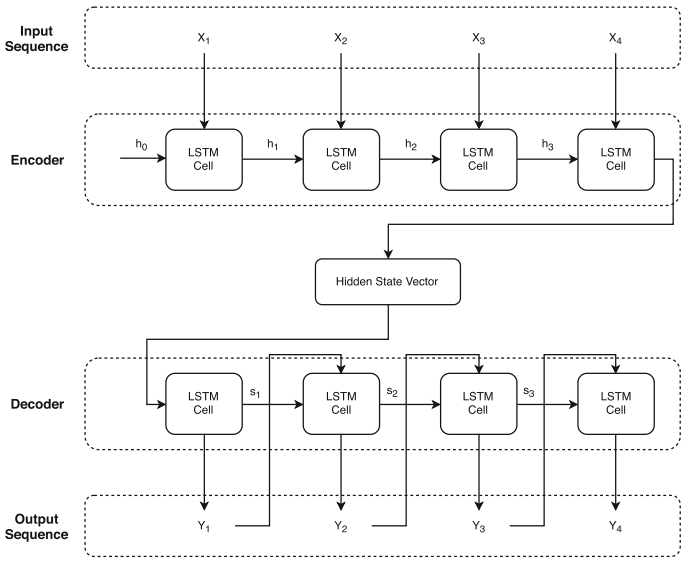

Fig. 1. Proposed Track Forecasting Model Architecture

3.3 Linear Typhoon Boundary Layer Wind Field Model

A linear height-resolving wind field model [21] is employed to generate the typhoon boundary layer wind field. The typhoon boundary layer wind fields are governed by 3D Navier-Stokes equations:

$$\frac{\partial \boldsymbol{v}}{\partial t} + \boldsymbol{v} \cdot \nabla \boldsymbol{v} = -\frac{1}{\rho}\nabla p - f\boldsymbol{k} \times \boldsymbol{v} + \boldsymbol{F} \tag{8}$$

where $\boldsymbol{v}$ is the wind velocity, f is the Coriolis parameter, $\boldsymbol{k}$ is the unit vector in the vertical direction, ρ is the air density, $\boldsymbol{F}$ is the frictional force, and p is the pressure. The pressure is calculated using the Holland pressure profile [22]:

$$p = p_c + \Delta p \exp[(-\frac{r_m}{r})^B] \tag{9}$$

where p_c, Δp, r_m, and B stand for central pressure, central pressure difference, radius to maximum winds, and Holland's B parameter, respectively.

The wind velocity $\boldsymbol{v}$ is expressed as a sum of the gradient wind velocity $\boldsymbol{v_g}$ and the frictional component $\boldsymbol{v'}$:

$$\boldsymbol{v} = \boldsymbol{v_g} + \boldsymbol{v'} \tag{10}$$

In a cylindrical coordinate system (r, θ, z), the gradient wind can be decomposed into the radial velocity v_{rg} and the azimuthal velocity $v_{\theta g}$. The radial component v_{rg} is often disregarded due to its insignificant effect, and the azimuthal component $v_{\theta g}$ can be expressed as:

$$v_{\theta g} = \frac{-c\sin(\theta - \nu) - fr}{2} + \sqrt{\frac{(-c\sin(\theta - \nu) - fr)^2}{4} + \frac{r}{\rho}\frac{\partial p}{\partial r}} \tag{11}$$

where c is the translation speed of the typhoon and ν is the heading direction of the typhoon.

The frictional component $\boldsymbol{v'}$ is solved with the boundary conditions:

$$\boldsymbol{v'}|_{z' \to \infty} = 0 \tag{12}$$

$$\rho K \frac{\partial \boldsymbol{v'}}{\partial z}|_{z'=0} = \rho C_d |\boldsymbol{v_s}| \boldsymbol{v_s} \tag{13}$$

where $\boldsymbol{v_s}$ is the wind velocity near the ground surface, and C_d is the drag coefficient. In this study, the scale analysis method described in [21] is adopted to obtain the frictional component u' and v'.

The wind field model is capable of calculating the wind speed of given locations near the typhoon center. The geographic coordinates of the observation locations and the first step output are combined as the input of the linear wind field model. The wind speed at the observation locations is then calculated as the prediction results of the proposed approach. Figure 2 illustrates the overall workflow of the proposed method.

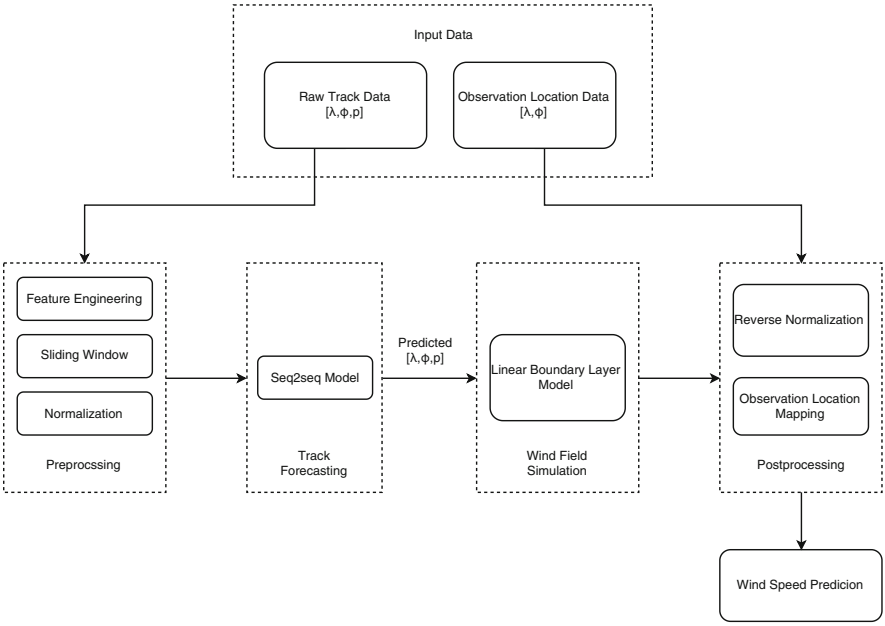

Fig. 2. Work flow of the proposed method

4 Case Study

4.1 Case Description

The case study considers the Guishan offshore wind farms (22.155N, 113.732E) as the observation locations. In this case study, the 10-min maximum sustained wind speeds observed at the Guishan offshore wind farms are used as ground truth values for the predictions. Typhoon Higos (2020) is the only typhoon that had a direct impact on the Guishan offshore wind farms after the wind farms were built. Therefore the case study only considers the wind speeds when typhoon Higos hit the Guishan offshore wind farms (2020-8-18 6:00 to 2020-8-19 12:00). The proposed model is implemented using Python [23] and Tensorflow [24] on a machine equipped with an NVIDIA GeForce RTX 3090 GPU.

The input data is derived from the CMA best track dataset using the preprocessing method described in Sect. 2. The track data of typhoon Higos is excluded from the training dataset to make fair predictions. Since the proposed model predicts the wind speed of the next four time steps, the following four different cases are implemented to test the performance of the individual prediction time steps:

- 6-h predictions: only use the first time step of each prediction as the prediction results. By doing so, the model is only able to make predictions 6-h ahead.
- 12-h predictions: use the first two time steps of the first prediction and the second time steps of the later predictions as the prediction results. The first

prediction of this case is 6-h before the first prediction of the 6-h predictions case. This case demonstrates the performance of the second step of the predictions.
- 18-h predictions: use the first three time steps of the first prediction and the third time steps of the later predictions as the prediction results. The first prediction of this case is 6-h before the first prediction of the 12-h predictions case. This case demonstrates the performance of the third step of the predictions.
- 24-h predictions: use the first four time steps of the first prediction and the fourth time steps of the later predictions as the prediction results. The first prediction of this case is 6-h before the first prediction of the 18-h predictions case. This case demonstrates the performance of the fourth step of the predictions.

The evaluation criteria of the case study results includes root mean squared error (RMSE), mean absolute error (MAE) and the coefficient of determination (R^2):

$$\mathrm{RMSE} = \sqrt{\frac{1}{N}\sum_{1=1}^{N}(y_i^{\mathrm{pred}} - y_i^{\mathrm{true}})^2} \tag{14}$$

$$\mathrm{MAE} = \frac{1}{N}\sum_{1=1}^{N}|y_i^{\mathrm{pred}} - y_i^{\mathrm{true}}| \tag{15}$$

$$\mathrm{R}^2 = 1 - \frac{\sum_{1=1}^{N}(y_i^{\mathrm{pred}} - y_i^{\mathrm{true}})^2}{\sum_{1=1}^{N}(y_i^{\mathrm{pred}} - \overline{y}_i^{\mathrm{pred}})^2} \tag{16}$$

where y_i^{pred} denotes the predicted value and y_i^{true} denotes the ground truth value.

Table 1. Approximation Error

Model	6-h	12-h	18-h	24-h
RMSE (m/s)	4.6976	**2.0232**	3.9228	6.0110
MAE (m/s)	4.4172	**1.7489**	3.1820	5.2779
R^2	0.5358	**0.8250**	−0.0869	−3.0790

4.2 Performance Comparison

The prediction results are plotted in Fig. 3. The RMSE, MAE and R^2 of the different cases are shown in Table 1. Since the hidden states are passed through time steps in the seq2seq model, the approximation error will also accumulate through the steps. Therefore the errors are expected to be larger in further time steps. However, the results show that the 12-h predictions yield the best results.

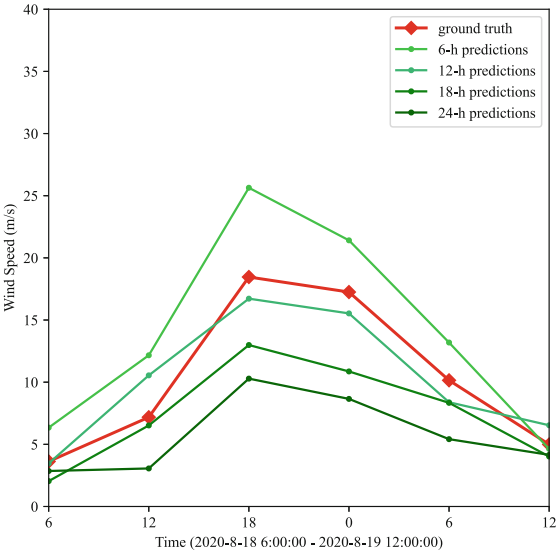

Fig. 3. Observed and simulated wind speeds at Guishan offshore windfarm during typhoon Higos (2020).

This is because the wind field model tends to overestimate the wind speed under our model configuration. The exact values of the wind field model parameters, such as the Holland B parameter and the radius of maximum winds, are hard to obtain. Thus the results may vary under different configurations of these parameters. Overall, the 12-h predictions are more reliable than the 18-h and 24-h predictions. The results suggest that the 12-h ahead predictions best suit the wind speed prediction task.

5 Conclusion

This paper presents a two-step approach for forecasting wind speed at offshore wind farms during typhoons. A feature extraction method is applied to the raw input to extract explicit information about the typhoons before the data is fed into the model in the first step. The first step utilizes an LSTM-based seq2seq model to predict the typhoon track and intensity based on the initial typhoon conditions. In the second step, the wind speed at given offshore locations is calculated using a physics-based linear wind field model. The proposed approach is tested on real-world observation data collected from Guishan Offshore Wind Farms during typhoon Higos (2020). The results show that the proposed approach is capable of predicting the wind speed 12-h ahead during typhoons accurately. Since most of the historical typhoon track datasets only provide data at 6-h intervals, the model in this work only makes reasonable predictions at 6-h intervals. Nevertheless, the proposed model can be easily trained to make predic-

tions with smaller intervals when training data with smaller intervals is available. Further research will be conducted for improving the wind field model.

References

1. Musa, S.D., Zhonghua, T., Ibrahim, A.O., Habib, M.: China's energy status: a critical look at fossils and renewable options. Renew. Sustain. Energy Rev. **81**, 2281–2290 (2018)
2. Wang, X., Li, J.: Parametric study of hybrid monopile foundation for offshore wind turbines in cohesionless soil. Ocean Eng. **218**, 108172 (2020)
3. Global Wind Energy Council: Global wind report 2019. Technical report. Global Wind Energy Council (2020)
4. Shultz, J.M., Russell, J., Espinel, Z.: Epidemiology of tropical cyclones: the dynamics of disaster, disease, and development. Epidemiol. Rev. **27**(1), 21–35 (2005)
5. You, Z.J.: Tropical cyclone-induced hazards caused by storm surges and large waves on the coast of China. Geosciences **9**(3), 131 (2019)
6. NHC: National hurricane center forecast verification (2021). www.nhc.noaa.gov/verification/. Accessed 14 Aug 2022
7. Neumann, C.J.: An alternate to the hurran (hurricane analog) tropical cyclone forecast system. Technical report, National Hurricane Center (1972)
8. Emanuel, K., Ravela, S., Vivant, E., Risi, C.: A statistical deterministic approach to hurricane risk assessment. Bull. Am. Meteor. Soc. **87**(3), 299–314 (2006)
9. Vickery, P.J., Skerlj, P.F., Twisdale, L.A.: Simulation of hurricane risk in the U.S. using empirical track model. J. Struct. Eng. **126**(10), 1222–1237 (2000)
10. Côté, J., Gravel, S., Méthot, A., Patoine, A., Roch, M., Staniforth, A.: The operational CMC-MRB global environmental multiscale (GEM) model. Part I: Design considerations and formulation. Mon. Weather Rev. **126**(6), 1373–1395 (1998)
11. Leith, C.: Theoretical skill of Monte Carlo forecasts. Mon. Weather Rev. **102**(6), 409–418 (1974)
12. Mullen, S.L., Baumhefner, D.P.: Monte Carlo simulations of explosive cyclogenesis. Mon. Weather Rev. **122**(7), 1548–1567 (1994)
13. Krishnamurti, T., Correa-Torres, R., Rohaly, G., Oosterhof, D., Surgi, N.: Physical initialization and hurricane ensemble forecasts. Weather Forecast. **12**(3), 503–514 (1997)
14. Krishnamurti, T.N., et al.: Multimodel ensemble forecasts for weather and seasonal climate. J. Clim. **13**(23), 4196–4216 (2000)
15. Alemany, S., Beltran, J., Perez, A., Ganzfried, S.: Predicting hurricane trajectories using a recurrent neural network. In: Proceedings of the AAAI Conference on Artificial Intelligence, vol. 33, pp. 468–475 (2019)
16. Giffard-Roisin, S., Yang, M.: Deep learning for hurricane track forecasting from aligned spatio-temporal climate datasets. In: 32nd Annual Conference on Neural Information Processing Systems Workshop on Modeling and Decision-Making in the Spatiotemporal Domain (2018)
17. Ying, M., et al.: An overview of the China meteorological administration tropical cyclone database. J. Atmos. Oceanic Tech. **31**(2), 287–301 (2014)
18. Lu, X., et al.: Western north pacific tropical cyclone database created by the China meteorological administration. Adv. Atmos. Sci. **38**(4), 690–699 (2021)
19. Lambert, J.H., Tobler, W.R., Lambert, J.H.: Notes and comments on the composition of terrestrial and celestial maps. Department of Geography, University of Michigan (1972)

20. Hornik, K., Stinchcombe, M., White, H.: Multilayer feedforward networks are universal approximators. Neural Netw. **2**(5), 359–366 (1989)
21. Snaiki, R., Wu, T.: A linear height-resolving wind field model for tropical cyclone boundary layer. J. Wind Eng. Ind. Aerodyn. **171**, 248–260 (2017)
22. Holland, G.J.: An analytic model of the wind and pressure profiles in hurricanes. Mon. Weather Rev. (1980)
23. Van Rossum, G., Drake, F.L.: Python 3 Reference Manual. CreateSpace, Scotts Valley (2009)
24. Abadi, M., Agarwal, A., Barham, P., Brevdo, E., et al.: TensorFlow: large-scale machine learning on heterogeneous systems (2015). Software available from https://www.tensorflow.org/